Damping Associated with Incipient Melting in Aluminum-Indium Alloys.

O. Diehm, C.R. Wong*, and D.C. Van Aken

Department of Materials Science & Engineering
University of Michigan
Ann Arbor, MI 48109-2136

*David Taylor Research Center
Physical Metallurgy Branch
Code 2812
Annapolis, MD 21402-5067

Abstract

The strain amplitude dependent damping of binary aluminum-indium alloys containing nominally 0.6 to 17.3 weight percent indium was studied. A DuPont Dynamic Mechanical Analyzer model 983 was used to measure the damping capacity of these materials. Pure aluminum (99.99%) exhibited strain dependent damping at strain values as low as 70 με. The addition of 0.6 weight percent indium reduced the strain independent damping by a factor of 2, but the strain dependent damping was equivalent to that of the pure aluminum. Binary aluminum-indium alloys containing 4, 8, 12, and 16 weight percent indium exhibited a general increase in loss factor with increasing indium content; however, the strain dependent damping was no greater than that of the pure aluminum sample. No significant increase in damping was observed when the binary alloys were tested at temperatures above the melting point of indium. Two damping peaks were observed near the eutectic melting point when tested at 10 Hz and differential scanning calorimetry verified both of these peaks as due to the melting of the indium inclusions. It was concluded that the higher temperature damping peak was associated with smaller indium inclusions and that the damping peaks were related to the solute segregation associated with the binary eutectic reaction.

Introduction

The typical structural aluminum (Al) has a high stiffness, but a low specific damping capacity. The typical loss factor for a precipitation hardened Al- based alloy is between 10^{-3} and 10^{-4}. Metal matrix composites have shown increased damping [1] but these materials can not be considered high damping because they have loss factors less than 10^{-2} [2]. An alternate approach to the development of a high damping composite would be by the incorporation of a viscoelastic fiber in addition to the stiff fibers used for reinforcement. Thus, the matrix would provide the structural stiffness and the various fibers would provide the desired damping capacity and the added stiffness. Although the composite material would show a lower stiffness than the stiff metal matrix composite, the increase in damping capacity may be of greater importance.

Indium (In) is a viscoelastic metal with an ultimate tensile strength of 3.1 MPa (450 psi) at room temperature.The loss factor of In has been reported to vary from 0.06 at room temperature to 0.2 at 100°C [3]. The melting point of pure indium is 156 °C and when combined with Al forms an immiscible alloy system, as shown in the phase diagram in Fig. 1. An alloy of 17.3 weight percent In will solidify by a monotectic reaction ($L \rightarrow Al + L_2$) which produces a continuous Al-matrix with an In-rich (L_2) entrapped liquid. At 156 °C, the In-rich liquid will solidify by the eutectic reaction $L_2 \rightarrow Al + In$. This final eutectic reaction will normally produce inclusions which are single-phase, i.e. pure indium. The small weight fraction of Al produced during the eutectic reaction is "divorced" to the pre-existing Al-matrix. The resulting microstructure will consist of an Al-matrix with a dispersion of In inclusions.

It is the purpose of this paper to examine the effect of a viscoelastic inclusion, such as In, on the damping capacity of Al. It is expected that the composite microstructure will demonstrate strain dependent damping as a result of micro-plasticity (dislocation motion) within the inclusion. In addition, high temperature loss factor measurements will be used to determine the damping associated with liquid inclusions. It is also expected that the first order transformation (the eutectic reaction) at 156 °C will produce both an anomalous modulus effect and a frequency dependent loss peak. The following formula from Nowick and Berry[4] describes the relaxation time, τ, as a function of the radius, r, of the second phase particle for a two phase material during a first order transformation.

$$\tau = r^2 / 3 D Vf \qquad (1)$$

Where D is the diffusivity and Vf is the volume fraction of the second phase particle. It should be noted that the relaxation time will be strongly dependent upon the size of the second phase such that smaller particles would exhibit a shorter relaxation time.

Experimental Procedure

Binary Al-In alloys, with nominal compositions 0.6, 4, 6, 8, 12, and 16 weight percent In, were arc-melted in an argon gas atmosphere. These alloys were prepared from In, and Al, metals which each had a metallic purity better than 99.99%. The total weight of each arc-melted button was below 10 g to assure a homogeneous melt. The Al-17.3% In alloy was produced by induction melting in an argon gas atmosphere and was solidified at a slow rate using a ceramic insulator to produce a coarse distribution of In particles. Each sample was then cold-rolled 30%, annealed at a temperature of 532°C, and then cold-rolled and annealed again to produce a nominal sample thickness of 1mm. Rectangular-beam coupons

were cut from the rolled slab, using a diamond saw, to produce a sample shape with nominal dimensions 40 mm x 10 mm x 1 mm.

A DuPont Dynamic Mechanical Analyzer (DMA) model 983 was used to measure the damping response of the test coupons. At room temperature, and a fixed frequency of 0.1 Hz, the maximum strain amplitude was varied from 20 to 300 με by changing the oscillation amplitude and clamping distance between the pivot arms, see Fig.2. The driver arm produces a sinusoidal displacement inducing both a shear and bending stress. The damping capacity was measured as the loss factor which is equal to the tangent of the phase angle, tan δ, between the stress and the strain. Elevated temperature tests from 100 - 200°C were conducted at a strain amplitude of 70 με at both 1 Hz and 10 Hz. A heating ramp of 1 °C per minute and a helium gas atmosphere were used to minimize the temperature lag of the sample with respect to the furnace-controlling thermal couple. The eutectic melting temperature of the binary alloys was established using a Perkin-Elmer differential scanning calorimeter model 7.

Metallographic samples were prepared by mechanical polishing and etching in a hot aqueous solution of NaOH. Cross-sectional samples were cut to view the long transverse microstructures of the binary alloys. Electron microscopy studies were performed at The University of Michigan Electron Microbeam Analysis Laboratory. Thin foils for transmission electron microscopy were prepared by twin jet electropolishing in a solution of 20% nitric acid (by volume) and methanol.

Results

The room temperature damping results for the pure-Al and binary Al-In alloys are shown in Figs. 3 and 4. Each alloy exhibits a transition to a strain amplitude dependent damping at approximately 70 με. A comparison between the Al and the binary Al-0.6In alloy (all compositions are in weight percent) is shown in Fig.3. The addition of 0.6 In reduced the strain independent damping by a factor of 2, but the strain dependent damping was equivalent to that of the pure Al. The strain independent damping of the pure Al was also greater than the binary Al-In alloys, with the exception of the two highest In concentrations, i.e. Al-12In and Al-16In. In general, the damping capacity of the Al-In alloys increased with increasing In content, see Fig. 4. The microstructures exhibit elongated stringers of indium aligned parallel with the rolling direction as shown in Fig. 5.

The results of a typical 1 Hz temperature scan are shown in Fig. 6 for an Al-6In alloy. A first order transformation was observed between 160 and 170°C. The change in the storage modulus with respect to temperature shows an anomalous behavior in this temperature range. The eutectic melting temperature of 156 °C was verified by differential scanning calorimetry (DSC). However, the DSC results also revealed a second melting peak at 160 °C as shown in Fig. 7. Fig. 8 shows that both melting peaks were observed with the DMA during a 10 Hz temperature scan. The loss factor associated with this transformation did not vary significantly with respect to increasing the weight percentage of In as shown in Fig. 9. Although the total damping appears to increase with In content, the difference between the peak height and the background is nearly constant.

At the eutectic melting temperature, the binary alloys exhibit strain dependent damping as demonstrated by the Al-17.3In alloy in Fig. 10. This particular alloy had a coarse distribution on In particles due to its slow cooling rate from the melt. The temperature scan in Fig. 11 shows a large damping peak to background ratio at lower frequencies for the Al-17.3In alloy. When measuring the loss factor at the eutectic temperature for various

oscillation frequencies, the relative height of the peak was observed to increase from values of 0.002 at 1 Hz to 0.014 at low frequencies of 0.1 Hz.

Discussion

The strain dependent damping of the Al-In alloys appears to be associated with dislocation motion in both the Al-matrix and the In-particles. Thus, the damping of the Al-In alloys increases with increasing In content, but the total damping is less than that of the pure Al. This may indicate that the damping contribution from the matrix decreases with increasing In content. This effect may be explained if we associate the magnitude of the matrix damping with a mean-free-path of dislocation motion. Upon the addition of second phase particles, the mean-free-path of the dislocations will decrease in two ways: the In-particles will inhibit the grain size during annealing and the In-particles will act as dislocation traps. Both of these effects are a function of the volume fraction of the second phase. Therefore, the damping contribution from the matrix would be expected to decrease as the volume fraction of second phase is increased. A minimum would then be expected for the Al-In alloys since the damping contribution from the In-particles would increase with increasing volume fraction. This minimum is approximately at the Al-4In composition.

The addition of In also affects the strain independent damping of the Al-matrix, as shown in Fig. 3. Indeed, the addition of a very small amount of In (0.6%) reduces the loss factor to one-half that measured for pure Al, but this effect appears to be related to processing history. Electron microscopy studies have just begun to examine the differences in structure which results from the addition of In and the subsequent processing. For example, a second Al-0.6In alloy was processed with out annealing and the microstructure is shown in Fig. 12. The microstructure shows a fine subgrain structure with In particles on the subgrain boundary. However, this particular alloy shows a much higher loss factor. In fact, the loss factor measured for this sample was constant, with $\tan \delta = 0.016$, up to a strain amplitude of 150 $\mu\varepsilon$. Thus, further microstructural work is required before any conclusions can be made with regard to the strain independent regime.

The damping peak observed between 160 and 170°C is believed to be related to the eutectic melting temperature observed at 156°C by the differential scanning calorimeter. The difference in temperature is a reflection in the thermal lag associated with the DuPont DMA. The pivot arms are made of stainless steel and are in direct contact with the sample. Thus, the pivot arms act as a thermal reservoir with respect to the sample. This effect was minimized by flowing helium gas through the furnace as the temperature was ramped. The thermal lag for the Al-In samples varied between 4 and 10 °C.

Equation 1 provides a means to calculate the test frequency at which peak damping would be observed for a 2-phase microstructure going through a first order transformation. In the present case, the reaction is a eutectic where the In alloys with the surrounding Al-matrix to form a liquid. Self-diffusion of In in the liquid and in the solid state near the melting point is approximately 10^{-5} cm^2/s and 10^{-9} cm^2/s, respectively [5]. If the typical diameter of the In inclusion is taken as 2 μm, and a volume fraction of 0.02 is assumed, relaxation times of 170 and 0.017 seconds are expected using the self-diffusion rates for In in the solid and liquid states, respectively. This would correspond to test frequencies of approximately 0.01 Hz and 60 Hz for the solid and liquid states, respectively. Resolution of the damping peak was obtained at a test frequency of 0.1Hz, which would indicate an intermediate diffusivity. The diffusion rate of Al in In would be expected to be higher than the self-diffusion of In in the solid state since the atomic radius of Al is smaller than that of

In. Thus, a diffusivity between 10^{-7} and 10^{-8} cm^2/s may be reasonable. In terms of order-of-magnitude calculations, this would produce a relaxation time on the order of 10 seconds, or a test frequency of 0.1 Hz. The peak observed at the higher test frequencies may then be related to a smaller indium particle. It should be noted that the melting temperature of In is size dependent [6]. This effect is easily demonstrated by differential scanning calorimetry of an arc-melted Al-12In alloy, see Fig. 13. The moderate solidification rate will produce a fine structure of In particles which melt at a higher temperature. Upon cold-working, and subsequent annealing, the number of high melting In particles is reduced, as observed in the DSC results reported in Fig. 7.

Conclusions

The addition of In to Al exhibited a general increase in loss factor with increasing In content; however, the strain dependent damping was no greater than that of the pure Al sample. A precipitation hardening alloy would be more appropriate for evaluating the damping contribution resulting from the addition of a viscoelastic inclusion. No significant increase in damping was associated with liquid metal inclusions, but a large damping peak was observed which was associated with the eutectic transformation and the diffusion of Al solute in the In inclusions.

Acknowledgements

This work was sponsored by the Office of Naval Research and the Office of Naval Technology under contract 87-K-0452. The technical monitor was Dr. D.E. Polk. The authors are grateful for the assistance of Mr. Steve Miller in performing the differential scanning calorimetry.

References

1. A.K. Ray, V.K. Kinra, S.P. Rawal, and M.S. Misra, Role of Interfaces on Material Damping, eds. B.B. Rath and M.S. Misra, ASM International, (1985) p. 95.

2. D. Birchon, "Hidamets: Metals to Reduce Noise and Vibration", The Engineer, **22**, 207 (1966).

3. C.R. Wong, D.C. Van Aken, and O. Diehm, paper JDB of these proceedings.

4. A.S. Nowick and B.S. Berry, Anelastic Relaxation in Crystalline Solids, Academic Press, 1972, p. 485.

5. G.H. Geiger and D.R. Poirier, Transport Phenomena in Metallurgy, Addison-Wesley, 1980, p.458.

6. H. Saka, Y. Nishikawa, and T. Imura, "Melting temperature of In particles embedded in an Al matrix", Phil. Mag. A, 57, 895 (1988).

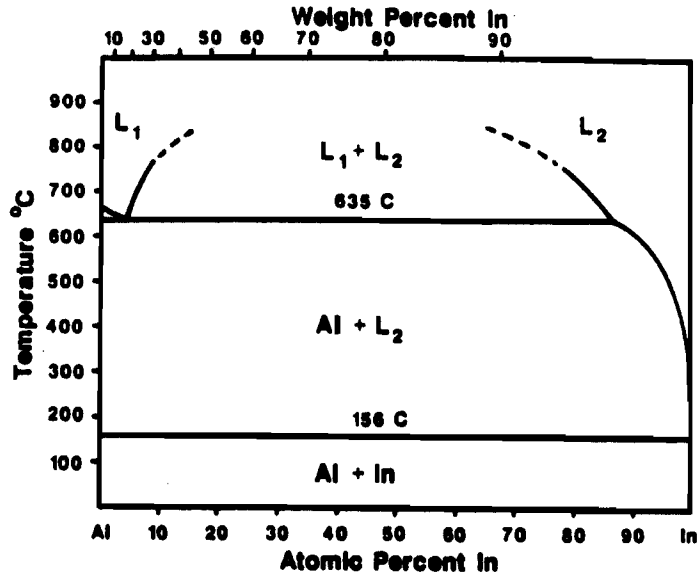

Fig. 1: Phase diagram of the Al-In binary system showing a liquid immiscibility gap.

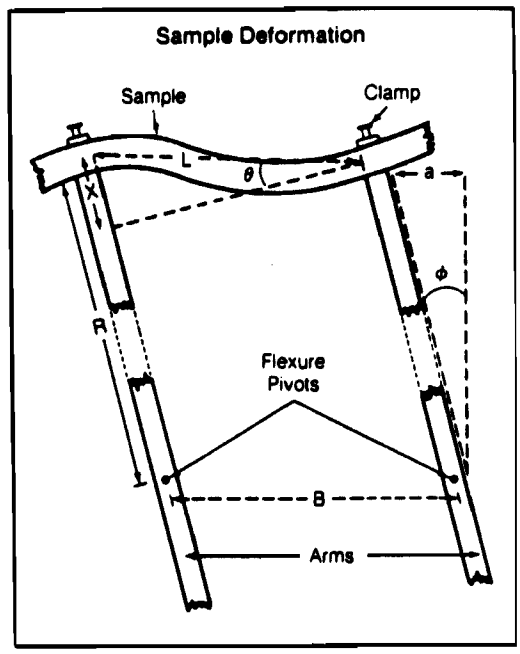

Fig. 2: Schematic representation of the pivot arm system for the DuPont DMA 983

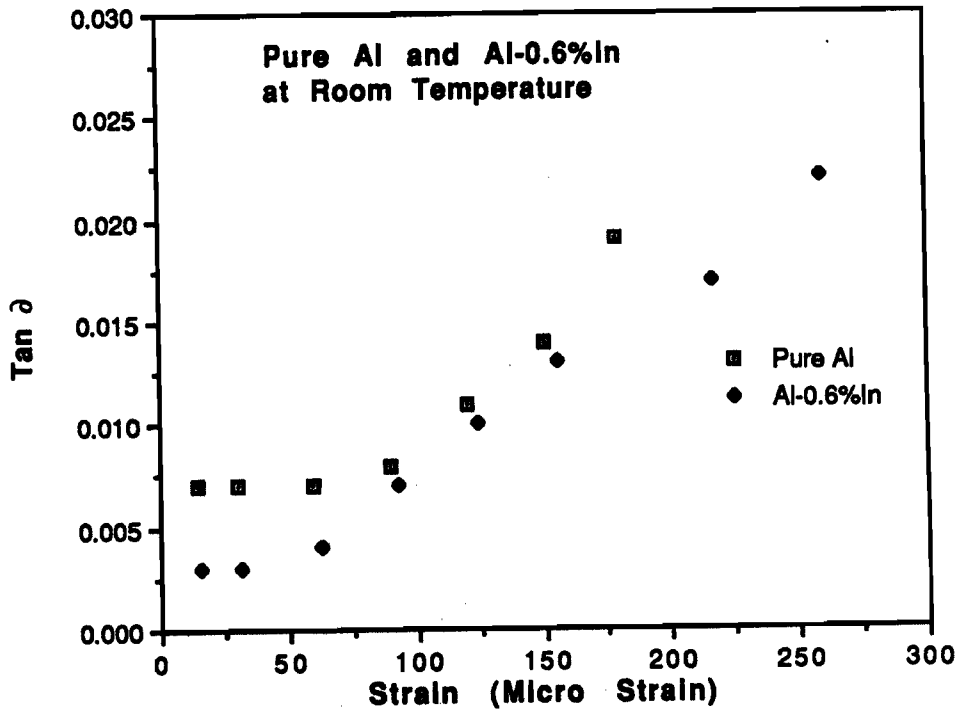

Fig. 3: Room temperature damping results of Pure Aluminum (99.99%) and Al-0.6In for various strain amplitudes.

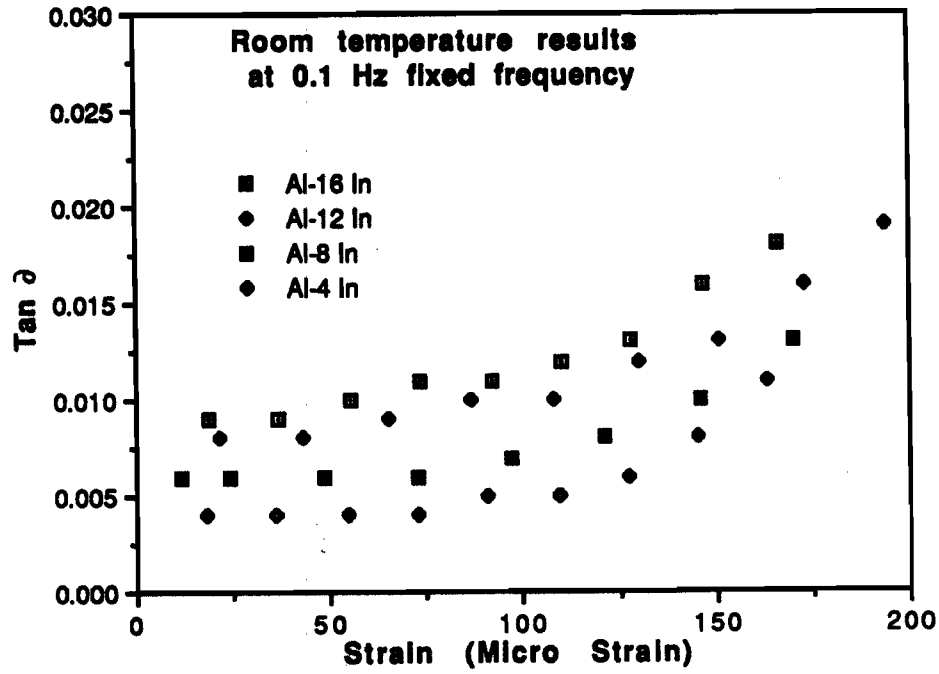

Fig. 4: Room temperature damping results of Al-4In, Al-8In, Al-12In, and Al-16In for several strain amplitudes.

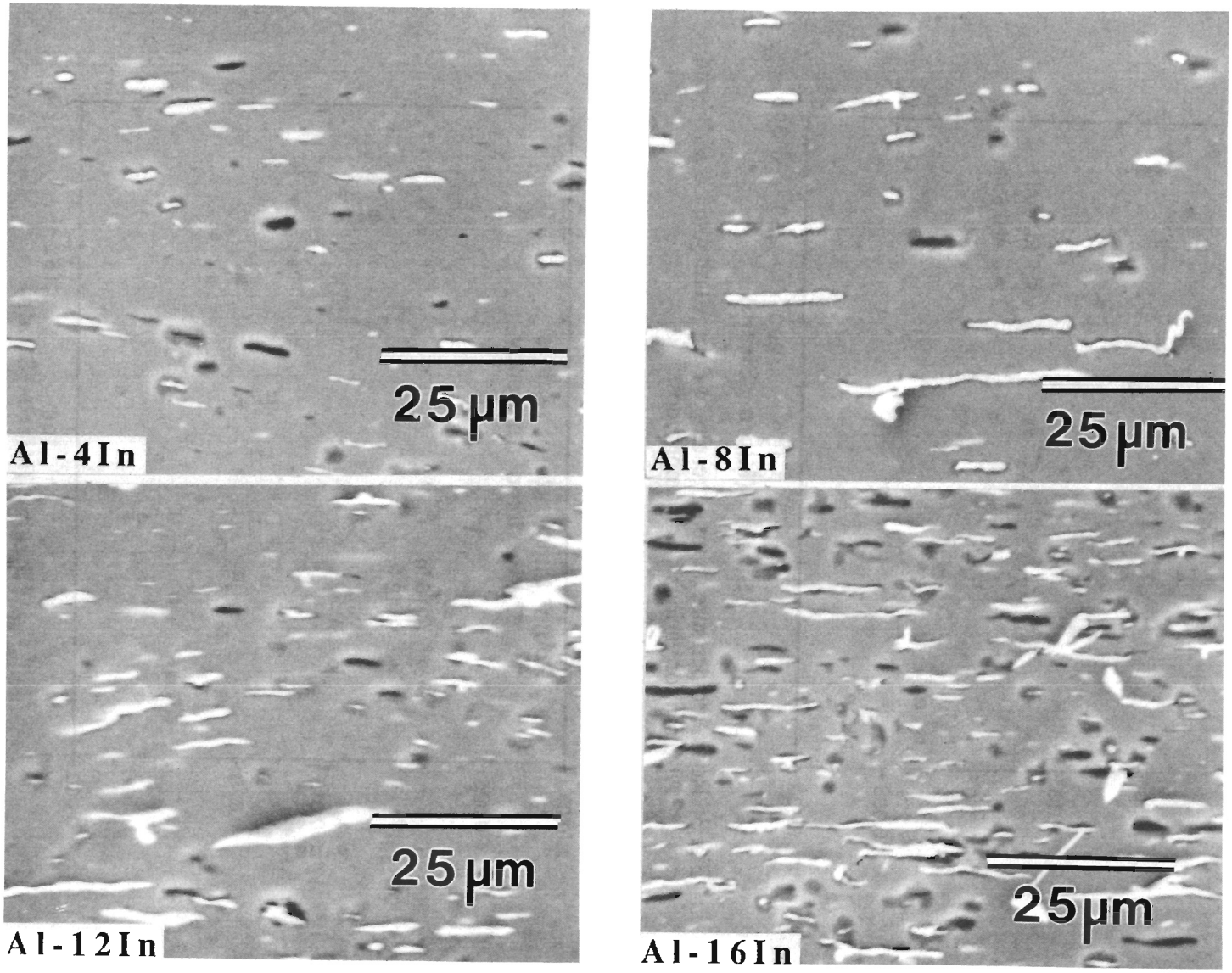

Fig. 5: Scanning electron micrographs of the Al-4In, Al-8In, Al-12In, and Al-16In alloys showing elongated indium stringers parallel to the rolling direction. The samples were polished and then etched in a warm aqueous solution of NaOH.

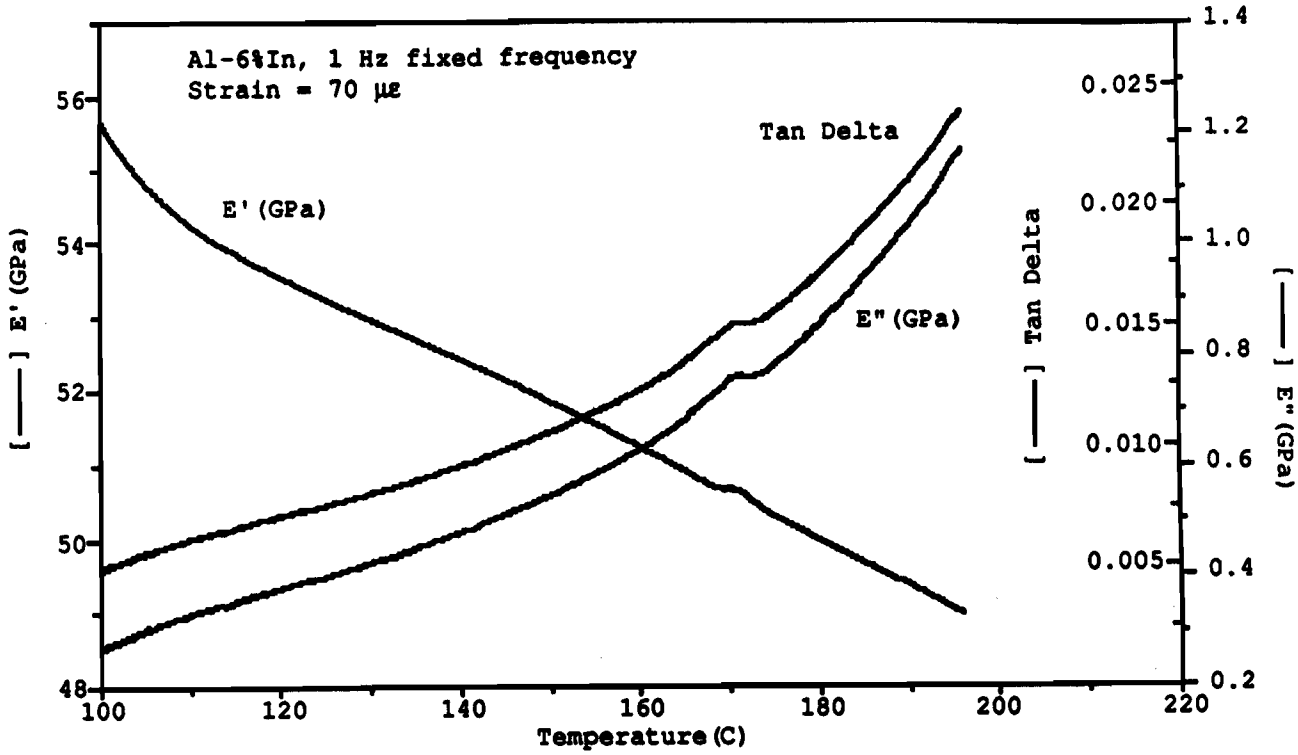

Fig. 6: Damping results from 100-200°C for the Al-6In alloy using a fixed frequency of 1 Hz and a strain amplitude of 70 με.

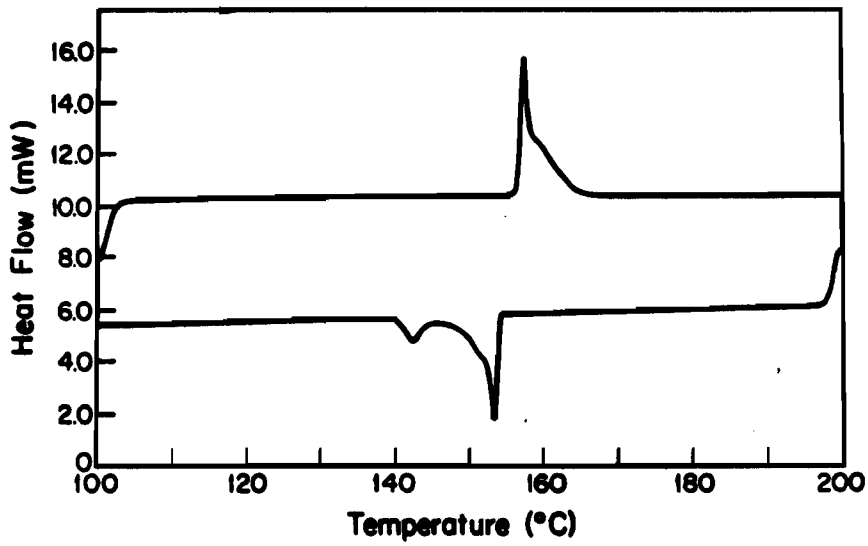

Fig. 7: Differential Scanning Calorimetry results from the Al-17.3In alloy exhibiting two melting peaks upon heating (top line) and three solidification peaks upon cooling (bottom line). The smallest peak (140°C) is associated with solid nucleation of the finest indium particles.

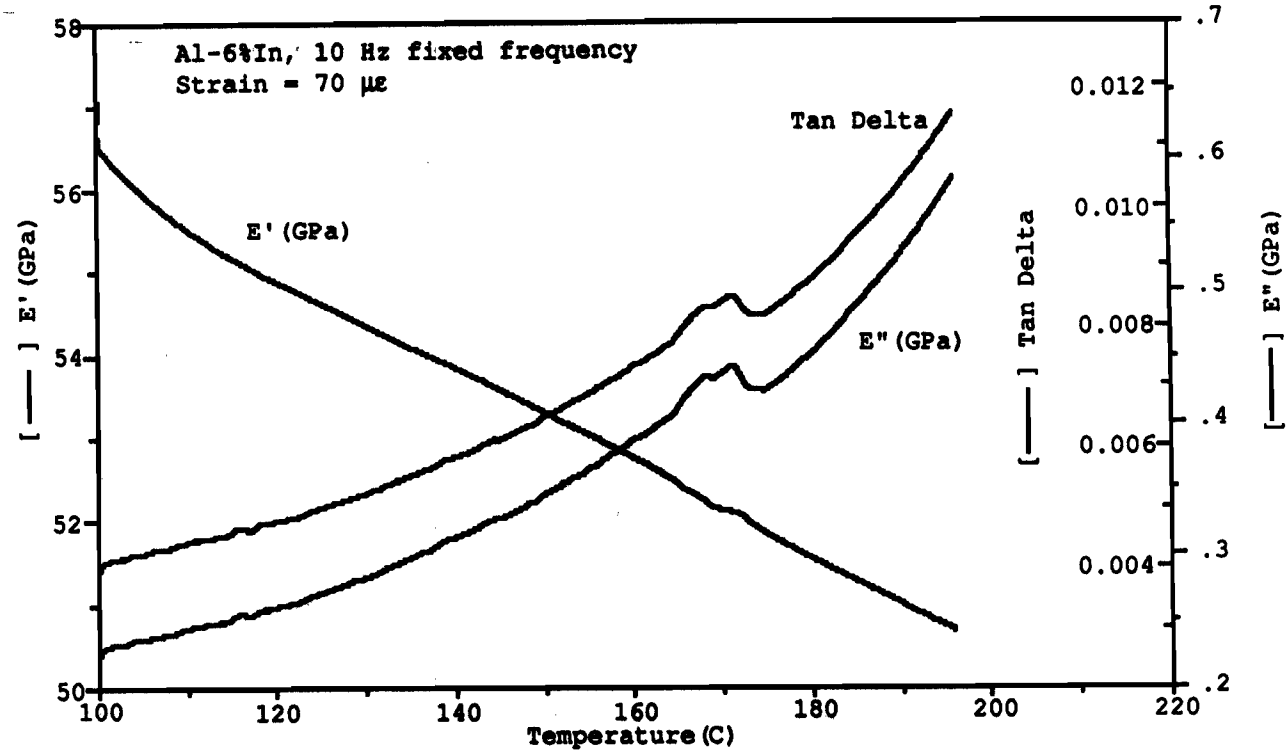

Fig. 8: Damping results for the Al-6In alloy at 10 Hz fixed frequency and strain amplitude of 70 με showing two distinct damping peaks.

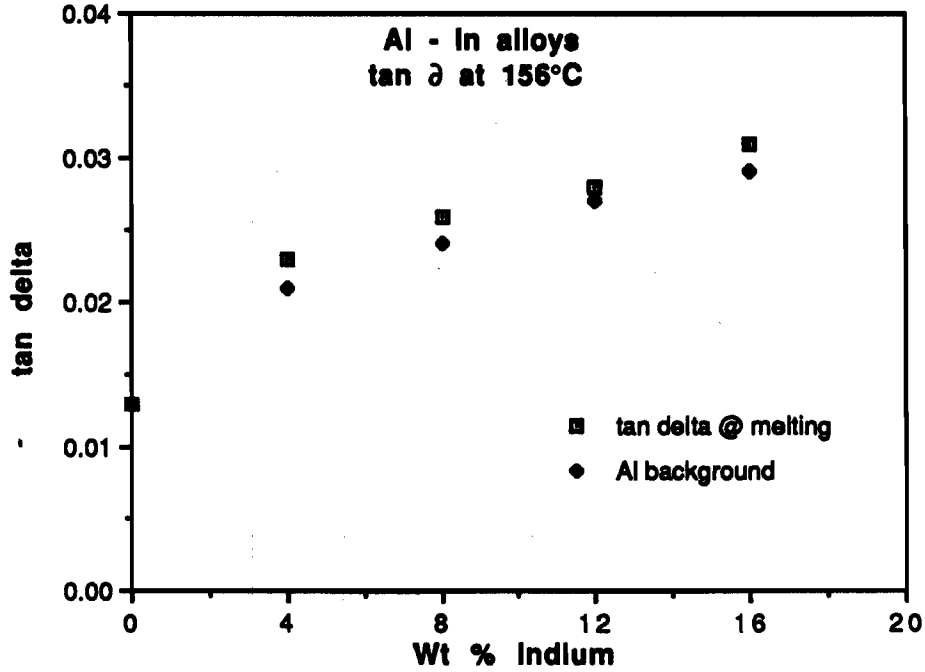

Fig. 9: DMA results indicating a slight increase of damping capacity at 156°C with increasing indium content and also showing damping contribution from the Al-matrix.

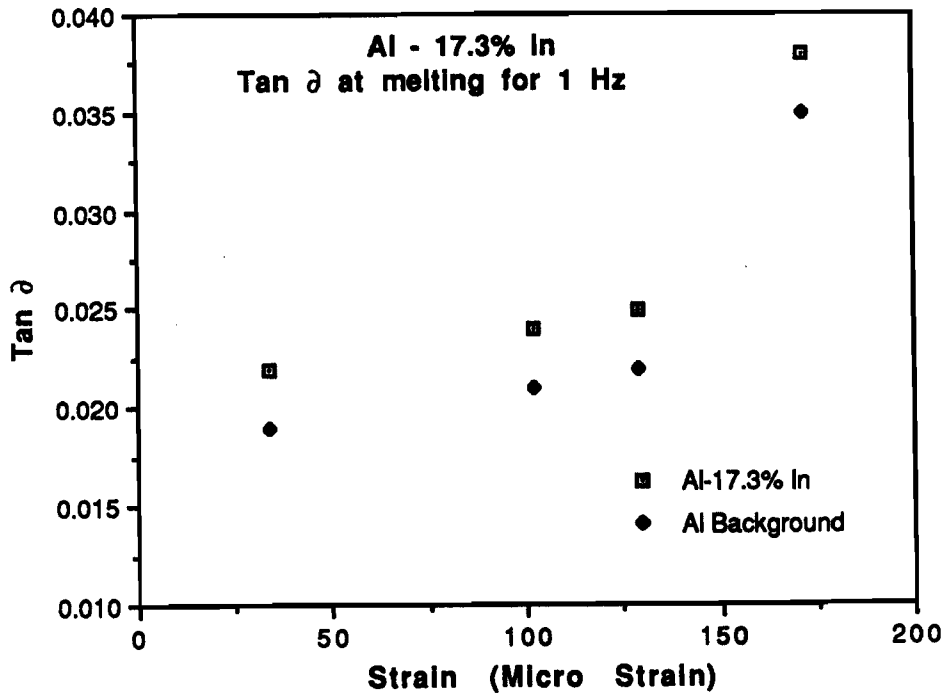

Fig. 10: Damping capacity results for the Al-17.3In alloy at 156°C at different strain amplitudes.

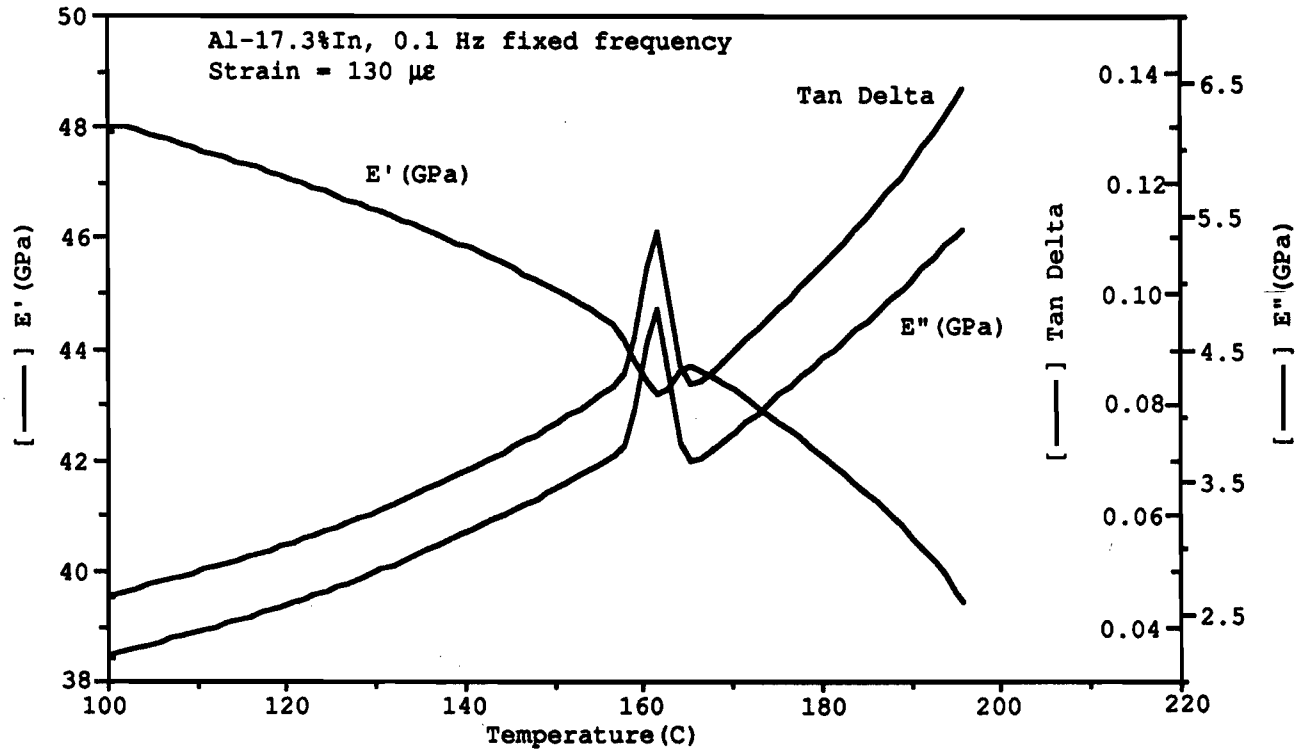

Fig. 11: DMA results for the Al-17.3In alloy at a frequency of 0.1 Hz demonstrating a larger damping peak to background ratio at lower frequencies.

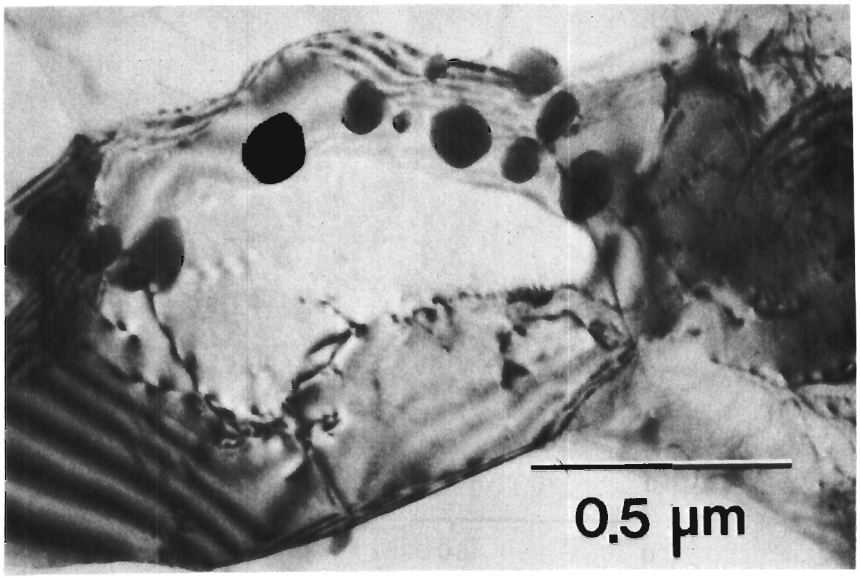

Fig. 12: Bright field transmission electron micrograph of the Al-0.6In alloy showing indium particles on a subgrain boundary.

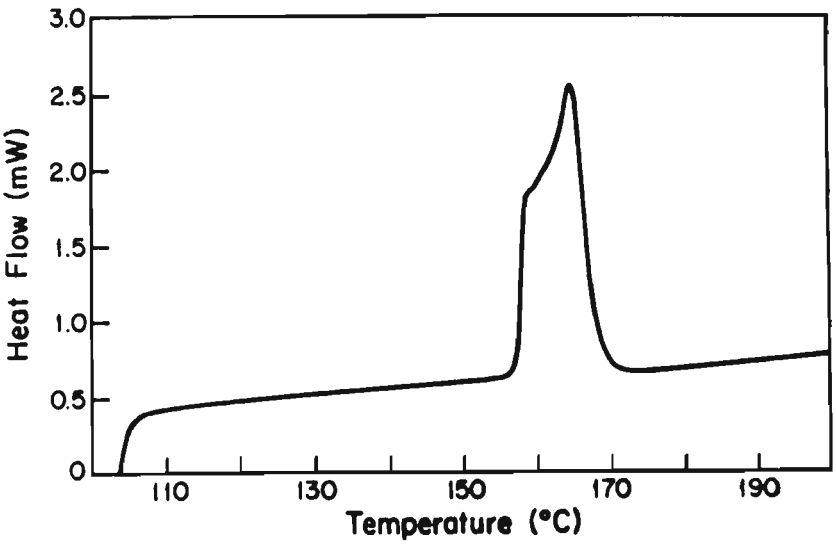

Fig. 13: DSC results for the Al-12In alloy indicating a second melting peak due to a fine structure of indium particles which melt at a higher temperature.